

# Predictive Prey Pursuit in a Whiskered Robot

Ben Mitchinson<sup>1</sup>, Martin J Pearson<sup>2</sup>, Anthony G Pipe<sup>2</sup>, and Tony J Prescott<sup>1</sup>

<sup>1</sup> ATLAS Research Group, The University Of Sheffield, UK

<sup>2</sup> Bristol Robotics Laboratory, Bristol, UK.

**Abstract.** Highly active small mammals need to capture prey rapidly and with a high success rate if they are to survive. We consider the case of the Etruscan shrew, which hunts prey including crickets almost as large as itself, and relies on its whiskers (vibrissae) to complete a kill. We model this hunting behaviour using a whiskered robot. Shrews strike rapidly and accurately after gathering very limited sensory information; we attempt to match this performance by using model-based simultaneous discrimination and localisation of a ‘prey’ robot (i.e. by using strong priors). We report performance that is comparable, given the spatial and temporal scale differences, to shrew performance in most respects.

## 1 Introduction

The Etruscan shrew must capture prey, sometimes not much smaller than the shrew itself (Figure 1), in twilight or dark conditions [1]. To that end, it relies on large facial whiskers (*macrovibrissae*) for both identification and localisation [2]. Whisker-triggered attacks on prey are highly spatially selective and may target an area that has not yet fallen within the whisker sensory field, indicating that they use a ‘Gestalt-like’ representation of the prey, functionally perceiving the whole prey despite sensing just part of it [2]. Shrew hunting has been described of consisting of four phases [3]: (i) pre-hunting, sessile, (ii) search, (iii) contact and (iv) attack (characterised by rapid head movement towards the prey). Whisker movements during phase (ii) [3] are similar to those seen in rat, mouse or opossum during un-motivated exploration [4]—that is, the whiskers are periodically swept forward and then backward in a movement known as a ‘whisk’. During phase (iii), whisker movement amplitude decreases whilst whisker protraction set-point may increase [3]; these results may be related to similar reports in rat [5].

We attempted to model this behaviour using our current whiskered robot, Shrewbot [7], pictured in Figure 1. Shrewbot cannot move as fast as the Etruscan shrew, so behaviour was slower than that seen in biological experiments

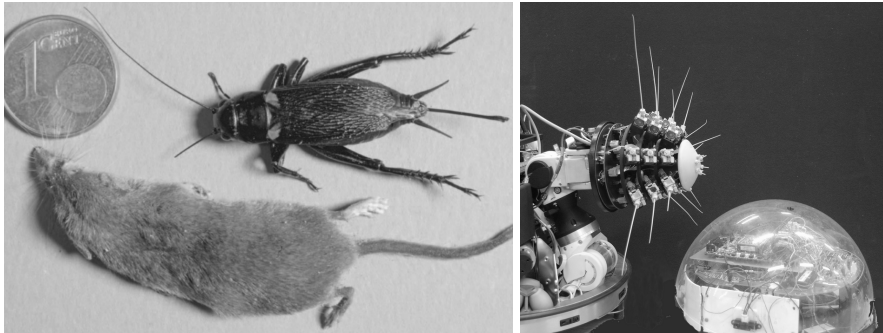


**Fig. 1.** (Left) Shrew and its prey, the cricket (reproduced with permission [2], Copyright (2006) National Academy of Sciences, USA). (Right) Shrewbot and its prey, Preybot.

(by about an order of magnitude). Whilst shrews appear able to rapidly perform reasonably nuanced discriminations [3], Shrewbot was tasked only with discriminating between Preybot (pictured) and flat or slightly curved vertical walls. We performed two experiments: Experiment 1 measured discrimination performance on the bench; Experiment 2 measured localisation performance of a stationary or moving target in the open field.

Discrimination performance on the bench for this binary task was almost perfect (perfect where contact was sufficiently robust); this performance was degraded in the open field, but remained fairly reliable. Localisation performance in the stationary case was good, with Preybot reliably located to well within a tenth of its diameter; this performance degraded only a little when the target was moving. Overall, our results illustrate that shape and surface orientation information carried across the time series recovered from multiple whiskers can be integrated and used to identify and locate a target in good time to drive behavioural responses. Moreover, they constitute a quantitative analysis of a problem analogous to that faced by the hunting shrew.

## 2 Models

Shrewbot’s (see Figure 1) electromechanical and control architecture is described at length elsewhere [6–8]. Briefly, it is based on a holonomic mobile platform (Robotino®, festo.com), has a bespoke three d.o.f. neck (elumotion.com), on the end of which is mounted the head, on which are mounted 18 mobile whiskers. Each whisker has 1 d.o.f. (rotation around its base, leading to ‘protraction’ or forward movement of its tip), and is instrumented for deflection in two axes

(denoted  $x$  and  $y$ ). From the length of this deflection vector we derive a ‘contact belief’ signal for the  $w$ th whisker,  $b_{\text{contact},w} = H(g_w(\|x, y\| - \eta_w))$ , where

$$H(a) = \begin{cases} 0, & a < 0 \\ 1, & a > 1 \\ a, & \text{otherwise.} \end{cases} \quad (1)$$

The parameters  $g_w$  and  $\eta_w$ , which vary with whisker length, are peripheral to this study and are not reported; they are chosen such that values of  $b_{\text{contact},w}$  of 0 and 1 correspond, approximately and respectively, to ‘certainty of not contact’ and ‘certainty of contact’. We can assume, here, that all software components are running at the same rate of 20Hz.

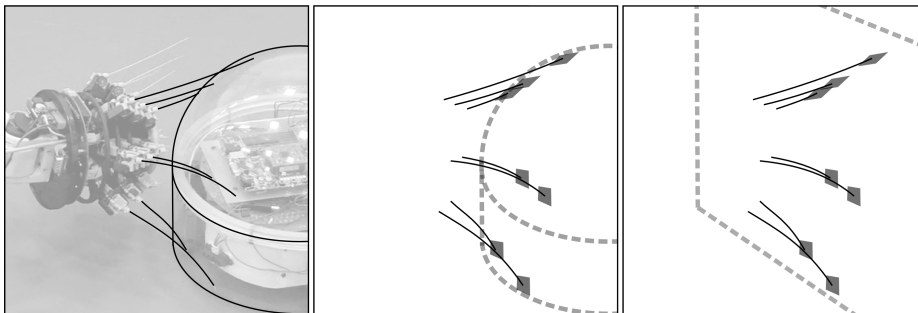


**Fig. 2.** Models and optimisation. (Left) Single frame from one trial shows Shrewbot bringing its whiskers forward to make as many contacts with Preybot as possible. Seven contacting whiskers are highlighted, as is Preybot. Two models are fitted to the contact data; Preybot ( $\mathcal{P}$ , middle) and a vertical wall ( $\mathcal{W}$ , right). Final model scores are penalised for surface location and orientation.

Owing to the morphology of Shrewbot, and the size of Preybot (300mm diameter), Shrewbot cannot sense more than a small part of the surface of Preybot at any one time. The model-based (or, ‘Gestalt-like’) approach to prey identification, suggested by the biology, provides both identity and position estimates simultaneously, despite this paucity of data (see Figure 2). Two models were fitted to the whisker data at each sample: one a model of a flat vertical wall ( $\mathcal{W}$ ), the other a model of Preybot ( $\mathcal{P}$ , a 150mm radius hemisphere atop a cylindrical base of 100mm height). The cost for each model ( $J_{\mathcal{W}}$  and  $J_{\mathcal{P}}$ , respectively) has two components: the first penalises contact locations that lay distant from the model surface; the second penalises whisker deflections that are in a different

direction to that expected given the local surface orientation at the contact location [9]. A time series called ‘prey belief’ is constructed from these cost values,  $b_{\mathcal{P}} = J_{\mathcal{W}}/(J_{\mathcal{W}} + J_{\mathcal{P}}) \in [0, 1]$ . An estimate of Preybot’s location (centre) relative to Shrewbot is also provided by the discriminator. The discriminator was hand-crafted according to the known geometry, using a linear model of whisker bending, and has only two free parameters ( $L$ , the number of samples over which to aggregate inputs, and  $w$ , the relative weighting of the second component of the cost function). Our only attempt to tune these was to manually and coarsely adjust  $w$  to optimise discrimination performance on the data from Experiment 1 ( $L$  was set, arbitrarily, to 5, for a 0.25s aggregation window).

An overhead camera was used to locate the robots with relatively low noise and no integral error. These data are combined with the relative Preybot location estimate provided by the discriminator to give two estimates of Preybot’s location (centre) in the 2D world-space defined in our experimental arena. These estimates, due to Shrewbot and to ‘ground truth’, are denoted  $\hat{s}_{\mathcal{P}}$  and  $s_{\mathcal{P}}$ , respectively. A velocity estimate is derived from each location estimate; these estimates are denoted, respectively,  $\hat{v}_{\mathcal{P}}$  and  $v_{\mathcal{P}}$ .  $\hat{s}_{\mathcal{P}}$  is boxcar-filtered (one second, causal) and combined with  $\hat{v}_{\mathcal{P}}$  assuming a constant prey velocity such that both  $\hat{s}_{\mathcal{P}}$  and  $\hat{v}_{\mathcal{P}}$  are smoothed but not lagged.  $s_{\mathcal{P}}$  and  $v_{\mathcal{P}}$  are not smoothed (and are not available to the robot, being used for analysis only).

When otherwise un-motivated, Shrewbot exhibits ‘explore’ behaviour, whereby it moves stochastically in a generally forward direction executing a whisk (forward-backward sweep of the whiskers) towards the end of each move. If it contacts something, it investigates it briefly, before moving back to explore behaviour. The details of this behaviour model, the **AttenSel** model described by [8], are peripheral to the current study. In the configuration used for Experiment 2, when  $b_{\mathcal{P}}$  rises above some threshold,  $b_{\mathcal{P}}^*$ , behaviour switches to ‘track’, whereby Shrewbot moves so as to bring Preybot into the whisker field on one or other side of the head such that many whiskers can be brought to bear on it (an example is shown in Figure 2). Since the location of Preybot in the whisker array is controlled (first-order positional control), Shrewbot effectively follows (‘tracks’) Preybot as it moves during this behaviour. Tracking behaviour continues to be exhibited until either  $b_{\mathcal{P}}$  falls below  $b_{\mathcal{P}}^*/2$ , or a fixed time (arbitrarily set to 4 seconds, for this report) has elapsed since tracking began—this tracking period allows the kinematic estimates to stabilise. In the former case, the trial is labelled a ‘refusal’ (R); in the latter case, the trial is labelled a ‘strike’ (S). In (S) trials,

a final behaviour is exhibited, denoted ‘strike’ (see below), and a two-second pause denoted ‘hold’ follows immediately after the strike. All trials analysed in Experiment 2 ended as either (R) or (S); a small number of trials were not analysed since no interaction between the robots occurred—these discards are noted, below. An example of this sequence of behaviours is provided below (Figure 5).

In (S) trials, Shrewbot completes the ‘prey capture’ by ‘striking’ at the ‘strike point’ on Preybot, a behaviour that executes in  $T_S = 0.8\text{s}$ . The strike point, denoted  $\psi$ , lies 120mm rearward of Preybot’s centre, and is marked with a white disc in figures and videos. Preybot is radially symmetric, so that  $\psi$  can only be identified uniquely if Preybot reveals its orientation by moving. If Preybot is stationary,  $\psi$  may lie anywhere around a circle 120mm from Preybot’s centre, and the point on this circle nearest to Shrewbot is targeted instead. One possible approach to integration would be to switch between these two behaviours based on the estimated Preybot speed; to avoid a discontinuity in behaviour, we chose instead to target a weighted average of these two estimates of the strike point, as follows. If Preybot is estimated to be moving ( $|\hat{v}_{\mathcal{P}}| \geq 80\text{mm/s}$ ), Shrewbot uses its estimates of Preybot’s location and velocity at time  $t$  to generate an estimate of  $\psi(t+T_S)$ , denoted  $\hat{\psi}_1(t+T_S)$ . If Preybot is estimated to be stationary ( $|\hat{v}_{\mathcal{P}}| = 0\text{mm/s}$ ), Shrewbot estimates  $\psi(t+T_S)$  to be 120mm along a line from  $\hat{s}_{\mathcal{P}}(t+T_S)$  towards the tip of Shrewbot’s snout at time  $t$ ; this estimate is denoted  $\hat{\psi}_0(t+T_S)$ . When the estimated speed is between these limits, a weighted estimate  $\hat{\psi} = \hat{\psi}_0 + |\hat{v}_{\mathcal{P}}|/80(\hat{\psi}_1 - \hat{\psi}_0)$  is used. Shrewbot then executes the ‘strike’, which places the tip of its snout (its ‘micro-foveal zone’, [8]) at  $\hat{\psi}(t+T_S)$  at time  $t+T_S$ . That is, this behaviour is predictive: the target reached is the expected location of the strike point at the end of the strike period. Thus, a successful strike (rendezvous-ing the tip of the snout and the strike point at the end of the strike period) is the culmination of successful identification, localisation, and velocity estimation. In the stationary case, of course, Shrewbot does not generally target the white disc at the end of the strike since  $\psi$  cannot be uniquely located.

Whilst expressing explore behaviour, movements of the head and transient protractions of the whiskers more-or-less alternate, so that the robot can be described as exhibiting ‘periodic whisking’ whilst exploring the world. During track behaviour, the whiskers undergo constant drive excitation, so that they are held strongly protracted. Working against this, transient negative feedback from  $b_{\text{contact},w}$  suppresses the drive to the corresponding whisker, according to the model described by [10]. As previously reported [11], the play-off between

this excitation and suppression often leads to rapid ‘palpation’ of the surface by contacting whiskers. This mix of excitatory and inhibitory influences may be a useful model of rat behaviour [12], and may act to maximize the number of contacts that occur whilst normalizing the depth of those contacts. The whisker movement that results during tracking has reduced amplitude and more protracted average angle, these being the main features described by [3] and [5].

### 3 Results

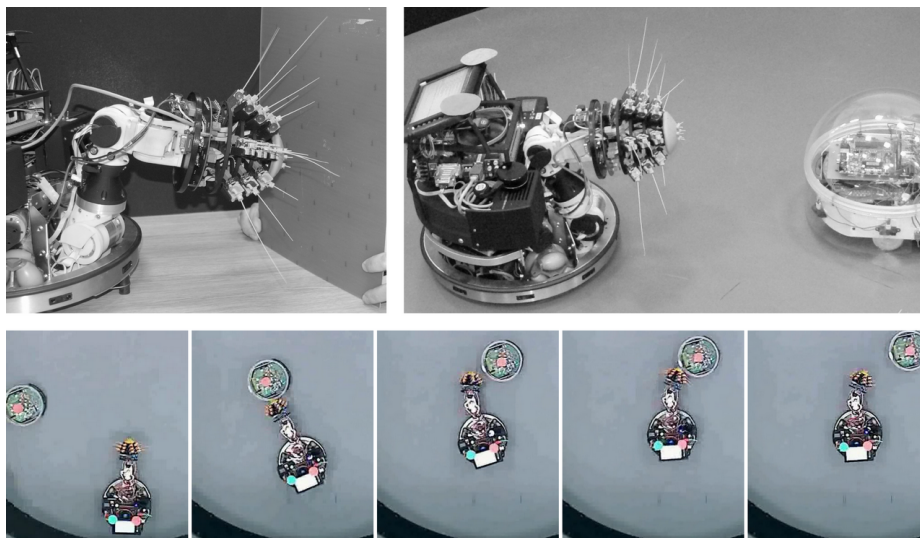


**Fig. 3.** Experimental set-up. (Top left) Experiment 1, experimenter presents a stimulus to an immobilised Shrewbot. (Top right) Experiment 2, Shrewbot approaches a stationary and helpless Preybot. (Bottom) Series of frames from overhead camera during (S) trial on a moving target. Frame times are  $t=0$  (trial begin), 6.7s (contact), 10.7s (begin strike), 11.5s (complete strike) and 13.5s (trial end).

#### Experiment 1: Discrimination

Experiment 1 was both a test of discrimination performance and our methodology to choose the discrimination threshold  $b_{\mathcal{P}}^*$ . We placed the robot on the bench and disabled the wheels, but allowed it to move its neck and whiskers freely, as if exploring. The experimenter presented one or other stimulus to the

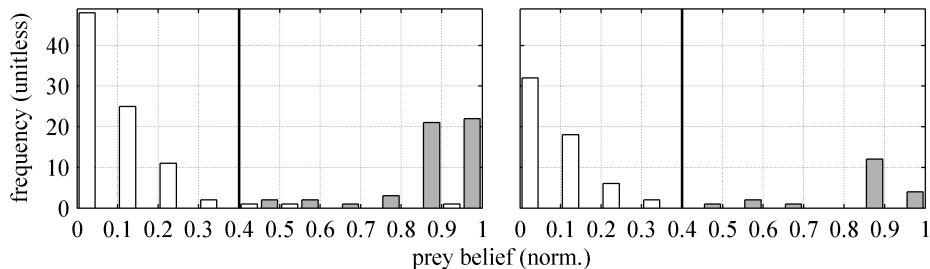


**Fig. 4.** Discrimination summary. Distribution of  $b_{\mathcal{P}}$  for (left) all 140 whisks in which contact occurred and (right) only those 78 whisks in which robust or multiple contacts occurred. Data for trials where prey was absent/present are shown using unshaded/shaded bars. Discrimination threshold  $b_{\mathcal{P}}^* = 0.4$  is shown as solid lines.

robot ( $\mathcal{W}$  or  $\mathcal{P}$ , see Figure 3). These presentations were intended to be varying but were not tightly controlled: on each whisk in the recorded dataset, the stimulus interacted with neither, one, or both whisker fields; the stimulus was stationary during some interactions and moving during others. The discriminator was active during this experiment, but its output was not used to change the behaviour of the robot, which continued to whisk, as if exploring, throughout. 245 whisks were collected, over 11 executions. From these, 140 whisks with some stimulus contact were identified (89/51 of these were  $\mathcal{W}/\mathcal{P}$ ). A value of  $b_{\mathcal{P}}$  was taken from each whisk at the point of maximum whisker protraction. We chose a discrimination threshold of  $b_{\mathcal{P}}^* = 0.4$ , by eye, to classify each stimulus into  $\mathcal{W}$  or  $\mathcal{P}$ ; classification performance is summarised in Figure 4. 3 errors were made over the 140 whisks (all 3 cases were  $\mathcal{W}$  being identified as  $\mathcal{P}$ , i.e. false positive prey identification). Including only those whisks where  $\sum_w b_{\text{contact},w} \geq 1.0$  (that is, firm contact on a single whisker or some contact on at least two whiskers), 78 whisks were included (58/20 were  $\mathcal{W}/\mathcal{P}$ ) and no errors were made.

## Experiment 2: Localisation

Experiment 2 was a test of discrimination, localisation, and velocity estimation, simultaneously. Shrewbot was positioned facing ‘North’ (along the +ve y-axis) and allowed to explore freely. In the first part of the experiment, Preybot was stationary somewhere ahead of Shrewbot (see Figure 3). Three locations were used, each for about one third of trials. In the second part, Preybot was moving on a trajectory that passed ahead of Shrewbot. Two classes of trajectory were used in about half of the trials each, one coming from each side of Shrewbot.

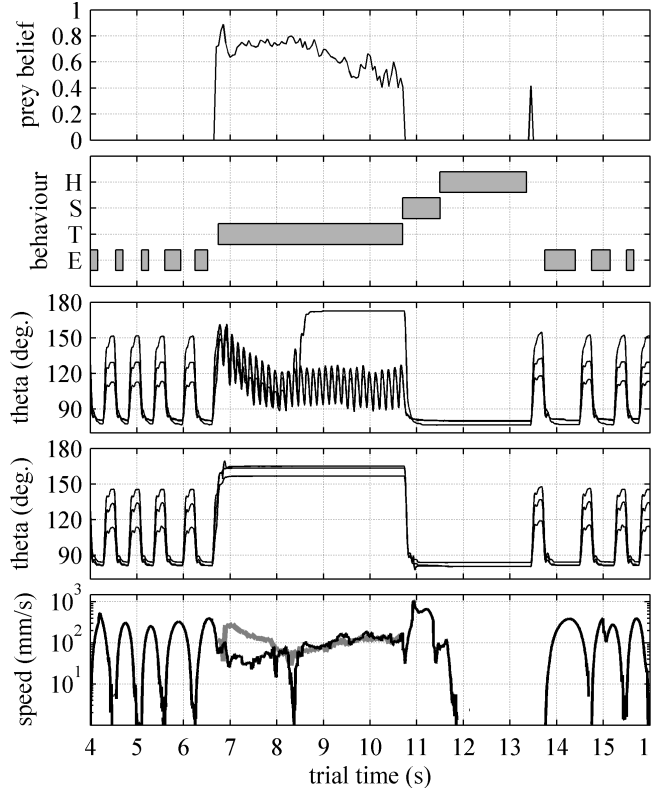


**Fig. 5.** Localisation example ethogram (moving target); each panel is against time within trial. (Panel 1, top) Prey belief,  $b_P$ . (2) Selected behaviour: (E)xplore, (T)rack, (S)trike, (H)old. (3/4) Whisker angles on the right/left (Preybot was tracked in the right hand side whisker array in this example). (5) Estimated prey speed (thick grey, unavailable when prey belief is zero) and Shrewbot snout movement speed (thin black).

Each individual trajectory had (roughly) constant velocity, and a speed of around 100mm/s. In those trials in which Shrewbot came into contact with Preybot, behaviour proceeded as described above, resulting either in a refusal (R) or a strike (S). Results from an example trial (moving target, (S) trial) are presented in Figure 5; results from all trials in Experiment 2 are summarised in Figure 6. Example overhead videos of trials are available: V1 ([goo.gl/6Tq0S](https://www.youtube.com/watch?v=6Tq0S), stationary target) and V2 ([goo.gl/QCSwR](https://www.youtube.com/watch?v=QCSwR), moving target, same trial as Figure 5 and lower part of Figure 3). 42 trials were recorded with Preybot stationary, of which 2 were discarded since the two robots did not interact. Of the remainder, 13 were refusals (R) and 27 were strikes (S), a false negative rate of about 1 in 3. The standard deviation (root mean square error) of Shrewbot’s estimates were



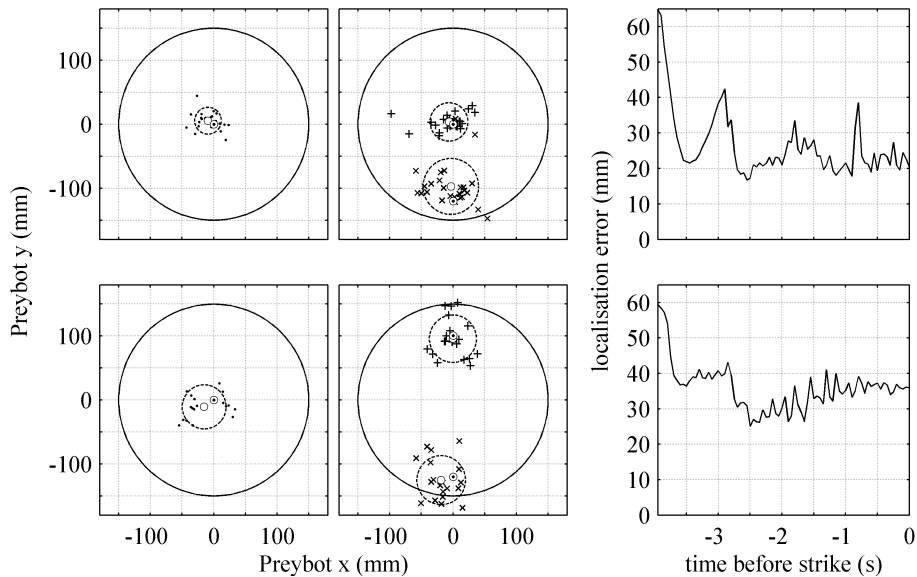


**Fig. 6.** Localisation summary. Two rows of three plots show results for stationary/moving target (upper/lower). The scatterplots present Shrewbot's estimates of Preybot location ( $\bullet$ , left-hand column), velocity and strike point ( $+$  and  $\times$ , middle column), each transformed into a coordinate system centred on Preybot (Preybot extents shown as solid circle). When Preybot is moving, its orientation is known; when it is not, it is assumed to be pointing 'North' (Shrewbot approaches roughly from 'South'). For each estimate, its true value ( $\odot$ ), measured mean ( $\circ$ ) and measured s.d. (dashed circle) is shown. The time series plots (to the right) display the error in Shrewbot's estimate of Preybot location (mean across trials), against time before strike.

21mm (23mm) for position, 30mm/s (30mm/s) for velocity, and 44mm (49mm) for strike point. 28 trials were recorded with Preybot moving; 2 were discarded since no interaction had occurred. The remainder comprised 7 refusals (R) and 19 strikes (S), a false negative rate of about 1 in 4. Standard deviation (root mean square error) of Shrewbot's estimates were 35mm (38mm) for position, 37mm/s (37mm/s) for velocity, and 38mm (42mm) for strike point.

## 4 Discussion

Shrewbot discriminated reliably between vertical walls and Preybot on the bench, and was fairly successful (65-75% success rate) at locking on to Preybot in the arena also. We did not formally test discrimination in the arena, but in informal testing false positives during interactions with walls were rare (data not presented). In (S) trials (successful strikes), localisation accuracy was much finer

than the size of Preybot itself. Across both conditions (stationary and moving target) and all three measures (position, velocity, future location of strike point) error can be summarised as being  $\sim 30\text{mm}$  or  $\sim 30\text{mm/s}$ , the diameter of Preybot being  $300\text{mm}$ . Altogether, our results illustrate how shape and surface orientation information carried across the time series recovered from multiple whiskers can be used to identify the what and where of a stimulus in good time to drive behavioural responses, at least for this case of only two discriminanda. Videos V3 (`goo.gl/HNoIn`) and V4 (`goo.gl/ppdCg`) are high-definition examples of (S) trials at  $100\text{mm/s}$  and  $150\text{mm/s}$ , respectively (a few trials were conducted at  $150\text{mm/s}$  but are not reported, here).

The temporal features of shrew hunting, as reported by [3], include periodic whisking near  $14\text{Hz}$  during search, and an average time between contact and attack of  $180\text{ms}$ . Shrewbot whisks at  $\sim 1.5\text{Hz}$  during search; whilst we allowed  $4\text{s}$  between contact and attack, graphing kinematic estimates against time (Figures 5 and 6) suggests that  $1.5\text{s}$  of data is probably adequate to stabilise them. Thus, Shrewbot operates around ten times less quickly than the shrew. Changes in direction during attack phase are detected by shrews and drive changes in attack trajectory with a latency as short as  $30\text{ms}$  [3]. Shrewbot currently retracts its whiskers during rapid movements (to protect them from damage) so that it cannot detect prey robot acceleration during this time; thus, this aspect of the response was not reproduced, here. At the Shrewbot timescale, around  $300\text{ms}$  would be available to detect a change in prey velocity and react accordingly; given the whisking rate during tracking of around  $7\text{Hz}$ , this is enough time for around two additional ‘samples’, so that reacting at this speed should be achievable. Shrews will make accurate attacks on stationary crickets [2], so that motion seems not to play a role in identification or orientation. In our paradigm, we used motion direction as a proxy for other features of the discriminandum that might reveal its orientation, but this is not a requirement of the approach.

In other recent work [8], we are exploring the hypothesis that much of the behaviour of small mammalian tactile specialists can be understood as foveation, the fovea in this case being the region around the mouth [15]. This hypothesis can be summarised by the statement that *foveation is action* for these mammals, since the primary actuators (teeth, tongue) are co-located with the primary sense organs (teeth, lips, tongue, nostrils, microvibrissae). Accordingly, the current behavioural model shares the architecture of oculomotor foveation control models—see Figure 7. Lower-level realisations of these oculomotor models

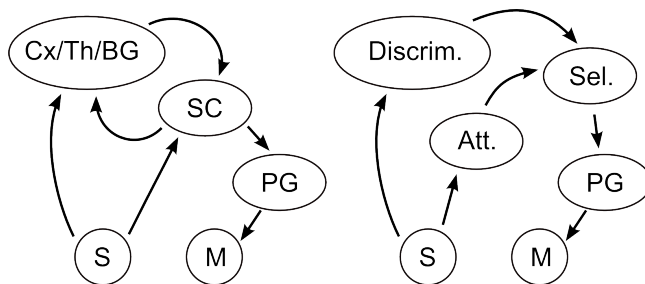


**Fig. 7.** Model. (Left) Essential organisation of contemporary (e.g. [13, 14]) models of oculomotor control. Selection takes place in loops through Superior Colliculus (SC), Cortex, Thalamus and Basal Ganglia (Cx/Th/BG). (Right) Current model shares this architecture but does not represent selection dynamics—rather, hysteresis is used to select between exploratory-like and hunting-like behaviours. Shown are (Discrim)ination, (Att)ention and (Sel)ection. Both panels represent Sensory periphery (S), Motor periphery (M), and Pattern Generation (PG).

achieve control through integration between attention, selection and—thus—identification and assessment of salience [16]. Available data are consistent with an analogous model of tactile foveation [17, 18], which we are developing in other work. Here, we have presented a high-level (functional) model of these integrative processes, with simple hysteretical behaviour selection.

This work represents a first model of hunting behaviour in the Etruscan shrew. Fleshing out the model to more closely mimic the biology will involve several lines of enquiry which may be of interest to biologists and roboticists alike. One such is to move towards a lower-level description of behavioural selection and implementation, combining electrophysiological data (e.g. [17, 18]) with increasingly rich behavioural data (e.g. [3, 4]) from small mammals, and taking advantage of ongoing interest in models of oculomotor control [19]. This may quickly uncover to what degree snout movements of small tactile mammals are akin, in nature and/or substrate, to saccadic movements in visual mammals, perhaps offering a robust and accessible comparative model to sit alongside the oculomotor system. This work also represents a report of a complete ‘whiskered mobile robot system’, in the sense of a system that can discriminate different classes of object, and select appropriate behaviour to exhibit towards them.

**Acknowledgments** The authors would like to thank Jason Welsby and Harsimran Singh (Bristol Robotics Laboratory) for their contributions to Shrewbot and Preybot, respectively. Supported by the FP7 grant BIOTACT (ICT-215910).

## References

1. Roth-Alpermann, C., Brecht, M.: Vibrissal touch in the etruscan shrew. *Scholarpedia* **4**(11) (2009) 6830
2. Anjum, F., Turni, H., Mulder, P.G., van der Burg, J., Brecht, M.: Tactile guidance of prey capture in etruscan shrews. *Proc Natl Acad Sci USA* **103**(44) (2006) 16544–16549
3. Munz, M., Brecht, M., Wolfe, J.: Active touch during shrew prey capture. *Frontiers in behavioral neuroscience* **4**(191) (2010)
4. Mitchinson, B., Grant, R.A., Arkley, K., Rankov, V., Perkon, I., Prescott, T.J.: Active vibrissal sensing in rodents and marsupials. *Phil. Trans. R. Soc. B* **366** (2011) 3037–3048
5. Berg, R.W., Kleinfeld, D.: Rhythmic whisking by rat: Retraction as well as protraction of the vibrissae is under active muscular control. *J Neurophys* **89**(1) (Jan 2003) 104–117
6. Pearson, M.J., Mitchinson, B., Welsby, J., Pipe, T., Prescott, T.J.: Scratchbot: Active tactile sensing in a whiskered mobile robot. In: *Proceedings of From Animals To Animats 11*, Paris, 25–29 August. Volume 6226 of LNCS. (2010) 93–103
7. Pearson, M.J., Mitchinson, B., Sullivan, J.C., Pipe, A.G., Prescott, T.J.: Biomimetic vibrissal sensing for robots. *Phil. Trans. R. Soc. B* **366** (2011) 3085–3096
8. Mitchinson, B., Pearson, M.J., Pipe, A.G., Prescott, T.J.: The emergence of action sequences from spatial attention: insight from mammal-like robots. In: *Proceedings of Living Machines*, 9–12 July, Barcelona (*in press*). (2012)
9. Fox, C., Evans, M., Pearson, M., Prescott, T.J.: Tactile slam with a biomimetic whiskered robot. In: *Proceedings of IEEE International Conference on Robotics and Automation (ICRA)*. (2012)
10. Mitchinson, B., Pearson, M., Melhuish, C., Prescott, T.J.: A model of sensorimotor co-ordination in the rat whisker system. In: *From Animals to Animats 9: Proceedings of the Ninth International Conference on Simulation of Adaptive Behaviour*. (2006) 77–88
11. Sullivan, J., Mitchinson, B., Pearson, M., Evans, M., Lepora, N., Fox, C., Melhuish, C., Prescott, T.: Tactile discrimination using active whisker sensors. *IEEE Sensors Journal* **12**(2) (2011) 350–362
12. Mitchinson, B., Martin, C.J., Grant, R.A., Prescott, T.J.: Feedback control in active sensing: rat exploratory whisking is modulated by environmental contact. *Royal Society Proceedings B* **274**(1613) (2007) 1035–1041
13. Arai, K., Keller, E., Edelman, J.: Two-dimensional neural network model of the primate saccadic system. *Neural networks* **7**(6-7) (1994) 1115–1135
14. Chambers, J., Gurney, K., Humphries, M., Prescott, A.: Mechanisms of choice in the primate brain: a quick look at positive feedback. In: *Modelling Natural Action Selection: Proceedings of an International Workshop*. (2005) 45–52
15. Brecht, M., Preilowski, B., Merzenich, M.M.: Functional architecture of the mystacial vibrissae. *Behavioural Brain Research* **84** (1997) 81–97
16. Straube, A., Büttner, U., eds.: *Neuro-ophthalmology: neuronal control of eye movements*. S Karger Ag (2007)
17. Sahibzada, N., Dean, P., Redgrave, P.: Movements resembling orientation or avoidance elicited by electrical stimulation of the superior colliculus in rats. *J Neurosci* **6**(3) (1986) 723–733

18. Hemelt, M.E., Keller, A.: Superior sensation: superior colliculus participation in rat vibrissa system. *BMC Neuroscience* **8** (2007) 12
19. Gandhi, N.J., Katnani, H.A.: Motor functions of the superior colliculus. *Annu. Rev. Neurosci.* **34** (2011) 205–31